BIOCHEMISTRY
including biophysical chemistry & molecular biology

Article

pubs.acs.org/biochemistry

Structure–Function Relationship of *Vibrio harveyi* NADPH–Flavin Oxidoreductase FRP: Essential Residues Lys167 and Arg15 for NADPH Binding

Hae-Won Chung[†] and Shiao-Chun Tu*[,†,‡]

[†]Department of Biology and Biochemistry, University of Houston, Houston, Texas 77204-5001, United States

[‡]Department of Biochemical Science and Technology, National Taiwan University, Taipei, Taiwan, ROC

ABSTRACT: *Vibrio harveyi* NADPH–FMN oxidoreductase (FRP) catalyzes flavin reduction by NADPH. In comparing amino acid sequence and crystal structure with *Escherichia coli* NfsA, residues N134, R225, R133, K167, and R15 were targeted for investigation of their possible roles in the binding and utilization of the NADPH substrate. By mutation of each of these five residues to an alanine, steady-state rate analyses showed that the variants K167A and R15A had apparently greatly increased $K_{m,NADPH}$ and reduced $k_{cat}/K_{m,NADPH}$, whereas little or much more modest changes were found for the other variants. The deuterium isotope effects $^{D}(V/K)$ for (4R)-[4-^{2}H]-NADPH were markedly increased to 6.3 and 7.4 for K167A and R15A, respectively, indicating that the rate constants for NADPH and NADP^{+} dissociation were greatly enhanced relative to the hydride transfer steps. Also, anaerobic stopped-flow analyses revealed that the equilibrium dissociation constant for NADPH binding (K_d) to be 2.5–3.9 and 1.1 mM for K167A and R15A, respectively, much higher than the 0.4 μM K_d for the native FRP, whereas the k_{cat} of these two variants were similar to that of the wild-type enzyme. Moreover, the K167 to alanine mutation led to even a slight increase in k_{cat}/K_m for NADH. These results, taken together, provide a strong support to the conclusion that K167 and R15 each was critical in the binding of NADPH by FRP. Such a functional role may also exist for other FRP homologous proteins.

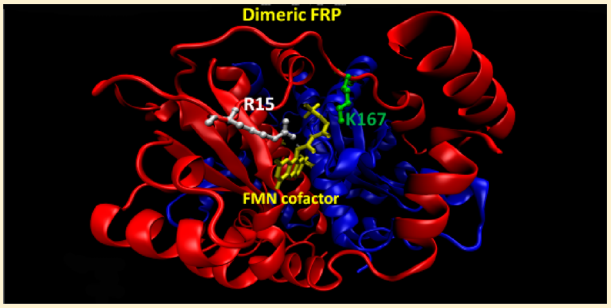

Reduced flavins participate in various biochemical processes, such as reduction of ferrisiderophores for iron release,[1] activation of the ribonucleotide reductase,[2] and reduction of methemoglobin.[3,4] In particular, reduced flavin serves as a substrate for monofunctional flavin-dependent monooxygenases.[5] The required reduced flavin is provided by NAD(P)H-flavin oxiodoreductases (flavin reductases), which catalyze the reduction of flavin by NAD(P)H. Each pair of a monofunctional flavin-dependent monooxygenase and its functionally linked, and often structurally associated, flavin reductase are referred to as a two-component monooxygenase couple.[5] Among such couples, the complex formation and activity coupling between flavin reductase and bacterial luciferase have been extensively studied.[6] Bacterial luciferase catalyzes the oxidation of reduced FMN ($FMNH_2$) and a long-chain aliphatic aldehyde (RCHO) by molecular oxygen to generate carboxylic acid (RCOOH), FMN, water, and light (λ_{max} 490 nm) (eq 1). The required $FMNH_2$ is produced by flavin reductases (eq 2).

$$FMNH_2 + RCHO + O_2 \rightarrow FMN + RCOOH + H_2O + light \quad (1)$$

$$FMN + NAD(P)H + H^+ \rightarrow FMNH_2 + NAD(P)^+ \quad (2)$$

Depending on the substrate specificity, flavin reductases are classified as three types.[5] Flavin reductase P (FRP) is specific for NADPH as a substrate and flavin reductase D (FRD) prefers the NADH substrate, whereas the general flavin reductase (FRG) utilizes NADPH and NADH with similar efficiencies.[7−10] For the *Vibrio harveyi* bacterial bioluminescence, the direct transfer of $FMNH_2$ from FRP to luciferase,[11,12] the complex formation between these two enzymes *in vitro*[13,14] and *in vivo*[14] have all been documented. The *frp* gene encoding *V. harveyi* FRP has been cloned, sequenced, and overexpressed.[15] The purified FRP comprises 260 amino acid residues (molecular mass 26 kDa) per monomer, which contains one noncovalently but tightly bound FMN cofactor.[15] FRP undergoes a monomer–dimer equilibrium in solution,[16] and the crystal structure at 1.8 Å resolution of the dimeric enzyme has been determined.[17] Structurally, the *V. harveyi* FRP is closely homologous to the *Escherichia coli* NfsA, which is a major oxygen-insensitive and NADPH-specific nitroreductase. NfsA and FRP share 51% identity in amino acid sequence, and both contain one FMN cofactor per monomer.[18] Superimposition of the FRP crystal structure with that of NfsA reveals a strong similarity despite

Received: February 19, 2012
Revised: May 9, 2012
Published: May 31, 2012

   dx.doi.org/10.1021/bi3002314 | *Biochemistry* 2012, 51, 4880–4887

```
nfsA   MTPTIELICGHRSIRHFTDEPISEAQREAIINSARATSSSSFLQCSSIIRITDKALREEL 60
snrA   MSPTIELLDGHRSIRHFTDEPVTEPQREAINCRARSTSSSSFLQCSSIIRITDRALREAL 60
frp    MNNTIETILAHRSIRKFTAVPITDEQRQTIIQAGLAASSSSMLQVVSIVRVTDSEKRNEL 60
nfra1  MNNTIETILNHRSIRSFTDQLLTAEEIDTLVKSAQAASTSSYVQAYSIIGVSDPEKKREL 60
       *. *** :  ***** **   ::  : :::   . ::*:** :*  **: ::*   :. *

nfsA   VTLTGGQKHVAQAAEFWVFCADFNRHLQICPD------AQLGLAEQLLLGVVDTAMMAQN 114
snrA   SCLTGGQKHVAQAAEFWVFCADFNRHLQICPD------AQLGLAEQLLLGVVDTAMMGQN 114
frp    AQFAGNQAYVESAAEFLVFCIDYQRHATINPD------VQADFTELTLIGAVDSGIMAQN 114
nfra1  SVLAGNQPYVEKNGHFFVFCADLYRHQQLAEEKGEHISELLENTEMFMVSLIDAALAAQN 114
         ::*.* :* . ..* *** *  **  :  :           :*  ::. :*:.: .**

nfsA   ALIAAESLGLGGVYIGGLRNNIEAVTKLLKLPQHVLPLFGLCLGWPADNPDLKPRLPASI 174
snrA   ALTAAESLGLGGVYIGGIRNNIESVTELLKLPKHVLPLFGLCLGWPAGNPDLKPRLPAEL 174
frp    CLLAAESMGLGGVYIGGLRNSAAQVDELLGLPENSAVLFGMCLGHPDQNPEVKPRLPAHV 174
nfra1  MSIAAESMGLGICYIGGIRNELDKVTEVLQTPDHVLPLFGLAVGHPANLSGKKPRLPKQA 180
          ****:***  ****:**.  * ::*  *.:   ***:.:* *   .  *****

nfsA   LVHENSYQPLD---KGALAQYDEQLAEYYLTRGSNNRRDTWSDHIRRTIIKESRPFILDY 231
snrA   VVHENQYQPLD---EKLLATYDEQLAEYYLTRGSNTRRDTWSDHIRRTLIKENRPFILEY 231
frp    VVHENQYQELN---LDDIQSYDQTMQAYYASRTSNQKLSTWSQEVTGKLAGESRPHILPY 231
nfra1  VYHENTYNVNTDDFRHTMNTYDKTISDYYRERTNGKREETWSDQILNFMKQKPRTYLNDY 240
       : *** *:         :  **: :  **  * .. : .***:.:   :  : *..:  *

nfsA   LHKQGWATR 240
snrA   LHKQGWATR 240
frp    LNSKGLAKR 240
nfra1  VKEKGFNKN 249
       ::.:*  ..
```

Figure 1. Sequence alignment of FRP[15] and homologous sequences from *E. coli* major nitroreductase (nfsA),[25] *Salmonella typhimurium* major nitroreductase (snrA),[19] and *Bacillus subtilis* nitro/flavin reductase (nfrA1).[20] The homologous sequences were acquired from the National Center for Biotechnology Information, and all sequences were aligned using ClustalW2. According to the definition from ClustalW2, asterisk (∗) is for fully conserved residue. Colon (:) and period (.) indicate partially conserved residues with strongly (scoring >0.5 in the Gonnet PAM 250 matrix) and weakly (scoring ≤0.5 in the Gonnet PAM 250 matrix) similar properties, respectively. Residues targeted for mutation were pointed by arrows.

the difference in using FMN and nitro compound, respectively, as their electron-accepting substrates.[18] Kobori et al.[18] proposed a model for binding of NADPH to NfsA by considering two minimum requirements. First, Arg203 should interact with the 2′-phosphate group of NADPH. Second, the nicotinamide ring of NADPH and the isoalloxazine ring of the FMN cofactor should be positioned close enough for hydride transfer.[18] Specifically, they proposed that Arg225, Arg133, and Asn134 interact with the nicotimamide moiety, and the positively charged side chains of Lys167 and Arg15 interact with the pyrophosphate of NADPH. In addition to the close similarities between the crystal structures of NfsA and FRP, the Arg15, Arg133, Asn134, Lys167, Arg203, and Arg225 are all conserved for these two enzymes and two other homologous enzymes, namely *Salmonella typhimurium* major nitroreductase (snrA)[19] and *Bacillus subtilis* nitro/flavin reductase (nfrA1)[20] (Figure 1). Moreover, we have previously shown that the Arg203 residue of *V. harveyi* FRP is indeed critical in NADPH binding by interacting with the adenosine 2′-phosphate of NADPH.[21] In order to explore further the structure−function relationship of *V. harveyi* FRP with respect to its preference for NADPH as a substrate, we set out to test the possible functional roles of Arg15, Arg133, Asn134, Lys167, and Arg225 by site-directed mutagenesis. Through multiple kinetic analyses of the purified mutated enzymes, the critical roles of Arg15 and Lys167 in NADPH binding were revealed.

■ EXPERIMENTAL PROCEDURES

Materials. Primers, $NADP^+$, NADPH, isopropyl β-D-1-thiogalactopyranoside, ethanol-d_6, aldehyde dehydrogenase from baker's yeast, and alcohol dehydrogenase from *Thermoanaerobium brokii* were all purchased from Sigma-Aldrich. BL21(DE3)pLysS competent cells were obtained from Stratagene. HiTrap DEAE FF, Superdex 75 10/300 GL, and Mono Q 5/50 GL columns were from GE Healthcare. A stock 1 M phosphate buffer solution was prepared with monobasic (KH_2PO_4) and dibasic (K_2HPO_4) at a molar ratio of 0.16/0.83. Dilutions with water to various degrees were made, and pH was adjusted to 7.0, if necessary, by the addition of either 4 M

dx.doi.org/10.1021/bi3002314 | *Biochemistry* 2012, 51, 4880−4887

H_3PO_4 or 5 M NaOH. Unless stated otherwise, 50 mM phosphate, pH 7.0, was used as the standard buffer.

Site-Directed Mutagenesis and Cell Growth. A pET vector harboring the wild-type *V. harveyi frp* gene, designated pFRP,[21] was used as a template for site-directed mutageneses using QuickChange lightning site-directed mustagenesis kit from Agilent Technologies. The primers used are listed in Table 1. The constructed mutant *frp* genes were verified by DNA sequencing (SeqWright). *E. coli* BL21(DE3) pLysS competent cells (Stratagene) were transformed with pFRP and FRP mutant plasmids and were inoculated at 37 °C overnight in 50 mL of LB broth containing 100 mg/L ampicillin (LBA). The overnight culture was transferred to 1 L of LBA and incubated in a thermostated shaker at 37 °C. Cells were grown until $OD_{600\ nm}$ reached around 0.8 and induced with 0.2 mM isopropyl β-D-1-thiogalactopyranoside. The cultures were further incubated in a thermostated shaker at 28 °C overnight and were harvested by centrifugation for 30 min at 8000*g*.

Table 1. Mutagenic Primers for FRP Variants[a]

mutant	primer
R15A	5′cttgctcatcgctctatc**gc**aaaattcaccgcagttcc3′
R133A	5′gcgtatatattggaggacta**gc**gaatagcgcagctcaagttg3′
N134A	5′gtatatattggaggactaagg**gc**tagcgcagctcaagttgatga3′
K167A	5′atcccgatcaaaatcccgaagta**gc**gccacgcctacc3′
R225A	5′gcttgctggtgagtcg**gc**acctcatattctgccg3′

[a]The mutagenic primers for FRP variants were designed using the QuickChange Primer Design Program from Stratagene. The bases modified to introduce the mutations are shown underlined and in boldface.

Purification of FRP Wild-Type and Variant Enzymes. The harvested *E. coli* BL21 cells expressing wild-type or mutated FRP were suspended in 35 mL ice-cooled lysis buffer [50 mM phosphate buffer pH 7.0 containing 1 mM ethylenediaminetetraacetic acid, 1 mM dithiothreitol (DTT), and 0.1 M NaCl]. The suspension was then sonicated on ice three times, each time for 8 min, and was subsequently centrifuged at 4 °C for 30 min at 14000*g*. In our earlier experiments we have observed that a significant part of the recombinant enzyme could be found in inclusion bodies. Therefore, the distributions of wild-type FRP and variants between soluble and inclusion body fractions were determined in each particular case by the following procedures. After centrifugation, the pellet was resuspended in the lysis buffer, sonicated, and centrifuged in order to further extract enzyme trapped in the pellet. Such a wash cycle was repeated two times. The supernatants from the first and second washes were combined. After the third wash, ~50 mg of the inclusion body pellet was resuspended in 1 mL of 1% sodium dodecyl sulfate solution and was analyzed, along with samples from the combined soluble phase, by sodium dodecyl sulfate−polyacrylamide gel electrophoresis.

For purification of wild-type FRP and variants found in the soluble fraction, the crude lysate of cells was filtered with 0.20 μm sterile syringe filter and loaded (flow rate 1 mL/min) on a DEAE-Sepharose FF column (1.6 × 2.5 cm) (GE Healthcare) pre-equilibrated with the standard buffer. The column was washed with the same buffer until the A_{280} baseline reached near zero, and fractions with significant enzymatic activities were obtained by elution (flow rate 3 mL/min) with 20 column volumes of a 0−0.5 M NaCl gradient in the standard buffer. The active fractions were concentrated to ~2 mL using an ultrafiltration centrifugal device with a 10 000 Da molecular weight cutoff (MWCO) membrane. The concentrated sample was loaded on a Superdex 75 10/300 GL (Tricorn) column (1 × 30 cm) pre-equilibrated and eluted with the standard buffer (flow rate 1 mL/min). The active fractions were loaded (flow rate1 mL/min) on a Mono Q column (0.5 × 5 cm) (GE Healthcare) pre-equilibrated and eluted the same way as for the DEAE-Sepharose FF column to obtain the highly purified FRP enzymes.

For FRP variants that were primarily found in inclusion bodies, their solubilization and purification followed the procedures as described previously[16,22] with minor modifications as described below. The inclusion body pellet after the third wash was suspended in 2 mL of 6 M guanidinium hydrochloride, 1 mM DTT, and 1 mM ethylenediaminetetraacetic acid in standard buffer. The suspension was gently stirred for 3 h at 4 °C and centrifuged at 14000*g* for 30 min. The supernatant was applied onto a Superdex 75 10/300 GL (Tricorn) column (1 × 30 cm) pre-equilibrated and eluted (0.5 mL/min) with 6 M urea and 1 mM DTT in standard buffer. Flavin reductase-containing fractions were collected and concentrated to about 2 mL using an ultrafiltration centrifugation device with MWCO 10 000 Da. The concentrated sample was mixed into 50-fold volume of precooled standard buffer containing 0.1 mM FMN and gently stirred on ice in the dark for 15 min. The sample was loaded on a DEAE-Sepharose FF column (0.5 × 5 cm) (GE Healthcare) pre-equilibrated and washed (flow rate 3 mL/min) with the same buffer until the A_{280} absorbance baseline reached near zero. Fractions with active FRP variants were obtained by subsequently eluting with 20 column volumes of a gradient of 0−0.5 M NaCl in the standard buffer.

Enzyme Assay and Kinetic Isotope Effect. All activity assays were carried out at room temperature in 1 mL of the standard buffer containing designated amounts of the wild-type or mutated FRP, FMN, and NADPH. Initial rates of NADPH oxidation (in ΔA_{340}/min) were measured using a Varian Cary 50 UV−vis spectrophotometer and converted to μM/min NADPH oxidation on the basis of ε_{340} = 6.2 mM^{-1} cm^{-1}. (4R)-[4-^{2}H] NADPH (NADPD) was prepared by following the Sem and Kasper's protocol[23] with minor modifications. 20 mM *N*-tris[hydroxymethyl]methyl-3-aminopropanesulfonic acid buffer containing 0.2 M ethanol-d_6, 5.6 mM $NADP^+$, and 1 mM DTT was incubated with 5 units/mL alcohol dehydrogenase and 1 unit/mL aldehyde dehydrogenase at pH 9.0. After 6−7 h, the reaction was quenched by adding several drops of CCl_4. After the reaction solution was separated into two layers, the aqueous layer was loaded onto a DEAE-Sepharose FF column pre-equilibrated and eluted with the standard buffer. After the A_{280} in eluate reached near zero, elution was continued with 20 column volumes of a gradient of 0−0.5 M NaCl in the standard buffer (flow rate 3 mL/min). (4R)-[4-^{2}H] NADPH was obtained from fractions having A_{260}/A_{340} < 2.41 and was used to replace NADPH in steady-state initial rate measurements for the determinations of deuterium isotope effect $^D(V/K)$

Anaerobic Stopped-Flow Measurements of Wild-Type FRP and FRP Variants. An FRP enzyme solution containing glucose oxidase (2% of the FRP enzyme concentration) (solution A) and an NADPH solution containing 1 mM glucose (solution B) were anaerobically prepared in a nitrogen-flushed glovebox at designated concentrations. Each solution was transferred to a glass syringe, leaving an open gas phase on

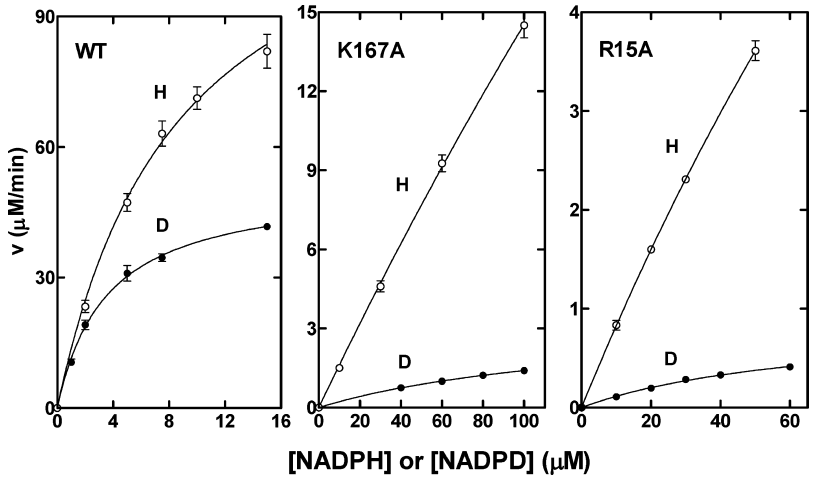

Figure 2. Initial velocities of wild-type FRP, K167A, and R15A as a function of NADPH or NADPD concentrations. Steady-state initial velocities were measured in 1 mL of 50 mM Pi standard buffer containing 50 μM FMN, various levels of NADPH or NADPD as indicated, and 2.7 nM FRP (left panel), 0.04 μM K167A (middle panel), or 0.06 μM R15A (right panel). The capital letters H and D are for NADPH (○) and NADPD (●), respectively. Initial velocities are normalized for all three panels on the basis of 0.1 μM enzyme per activity assay.

top of the solution in the syringe held at a tilted position. The solutions were made oxygen-free by blowing high-purity nitrogen gas for ~2 h over the solutions in the syringes. The syringes were sealed and transferred to an Olis rapid scanning monochromator stopped-flow apparatus, whose flow systems were prewashed once with a 50 mM dithionite solution and several times with an anaerobic standard buffer. Solutions A and B (125 μL each) were mixed, and changes in absorption at 450 nm (in a 1.6 cm light path flow cell) were monitored as a function of time.

RESULTS

General Kinetic Analyses. The *frp* and mutant genes were expressed in *E. coli* BL21 with isopropyl β-D-1-thiogalactopyranoside induction of T7 polymerase. After cell harvesting and lysis, FRP WT enzyme and variants N134A, R225A, and K167A were mainly found in the soluble fraction, whereas variants R15A and R133A were primarily recovered from inclusion bodies. All FRP enzymes were purified to ≥90% purities on the basis of sodium dodecyl sulfate−polyacrylamide gel electrophoresis patterns. The active FRP holoenzyme contains 1 FMN cofactor per monomeric enzyme.[15] The FMN cofactor contents in our isolated FRP WT enzyme, K167A, and R15A varied a little in different preparations but usually were in the range of 0.83 to 0.92 FMN per monomeric reductase. In all experiments, molar concentrations of wild-type FRP and variants were based on the contents of the FMN cofactor. In an initial series of FMN titration experiments at several fixed levels of NADPH, it was found that 50 μM FMN was saturating for wild-type FRP and all variants examined in this work. In subsequent experiments, enzyme initial velocities were measured as a function of NADPH concentration at a fixed level of 50 μM FMN to determine the $K_{m,NADPH}$, k_{cat}, and $k_{cat}/K_{m,NADPH}$ of FRP variants and compare them with those of the wild-type FRP. As reported previously,[12,15] activities of the wild-type FRP showed a typical Michaelis−Menten kinetic profile at increasing NADPH concentrations (Figure 2, left panel). Similar NADPH saturation curves were also found for R133A, N134A, and R225A. Double-reciprocal plots of initial velocities versus NADPH concentrations allowed the determination of $K_{m,NADPH}$, k_{cat}, and $k_{cat}/K_{m,NADPH}$ of these FRP enzymes, and results are summarized in Table 2. For all three kinetic parameters, R225A was quite similar to the wild-type reductase. On the other hand, R133A and N134A showed approximately 2- and 4-fold increases in $K_{m,NADPH}$, respectively, and 2.6- and 4.6-fold decreases in k_{cat}, respectively, in comparison with wild-type FRP (Table 2). Accordingly, the decreases in $k_{cat}/K_{m,NADPH}$ for R133A and N134A were 4.7- and 17.7-fold, respectively (Table 2).

Table 2. Steady-State Kinetic Parameters of Wild-Type FRP and Variants[a]

enzyme	$K_{m,NADPH}$ (μM)	k_{cat} (s^{-1})	$k_{cat}/K_{m,NADPH}$ (μM^{-1} s^{-1})
wild-type FRP	9 ± 1	23.8 ± 2.0	2.67 ± 0.50
R133A	16 ± 1	9.2 ± 0.3	0.57 ± 0.03
N134A	34 ± 4	5.2 ± 0.2	0.15 ± 0.02
R225A	10 ± 1	19.2 ± 0.7	2.00 ± 0.17
R15A	ND[b]	ND[b]	0.012 ± 0.001
K167A	ND[b]	ND[b]	0.025 ± 0.001

[a]Determined at a fixed concentration of 50 μM FMN and various levels of NADPH in 50 mM Pi, pH 7.0. [b]Not determined. See text for explanation.

Apparently, the $K_{m,NADPH}$ values for K167A and R15A were markedly increased. Up to 100 and 50 μM NADPH tested for K167A and R15A, respectively, their activities were very close to a linear function of NADPH concentration rather than a Michaelis−Menten saturation curve (Figure 2, middle and right panels). Hence, k_{cat} and $K_{m,NADPH}$ values for these two FRP variants could not be calculated individually. However, the initial linear portions of the activity versus NADPH plots as shown in Figure 2 allowed the determinations of 0.025 and 0.012 μM^{-1} s^{-1} as the $k_{cat}/K_{m,NADPH}$ values for K167A and R15A, respectively (Table 2), both being markedly slower than the 2.7 μM^{-1} s^{-1} for the wild-type FRP.

Deuterium Isotope Effect of K167A and R15A. Initial velocities of K167A, R15A, and wild-type FRP were also measured at a fixed 50 μM FMN and various levels of NADPD, and the results are shown in Figure 2. Values of $k_{cat}/K_{m,NADPD}$ were determined the same way as described above, and in comparison with results obtained with NADPH, the corre-

dx.doi.org/10.1021/bi3002314 | *Biochemistry* 2012, 51, 4880−4887

sponding values of deuterium isotope effect $^{D}(V/K)$ [i.e., $(^{H}k_{cat}/K_{m,NADPH})/(^{D}k_{cat}/K_{m,NADPD})$] were calculated to be 6.3 ± 1.6, 7.4 ± 0.3, and 1.0 ± 0.2 for K167A, R15A, and wild-type FRP, respectively.

Anaerobic Stopped-Flow Measurements of Reduction of K167A and R15A. Similar to wild-type FRP,[24] we found that the bound FMN cofactor of K167A and R15A could also be reduced by NADPH under anaerobic conditions. The rates of such reductions were determined by anaerobic stopped-flow measurements. When 10 μM K167A was reacted with 1 mM NADPH under oxygen-free conditions, absorption at 450 nm associated with the oxidized FMN cofactor decreased as a function of time (Figure 3, main figure). A replot of $\log(\Delta A/\Delta A_\infty)$ versus time is shown in the inset. The observed data (○) were fitted for a first-order process (dashed line) and for a process consisting of two consecutive reversible steps (solid line) as shown in the boxed portion of Scheme 1.

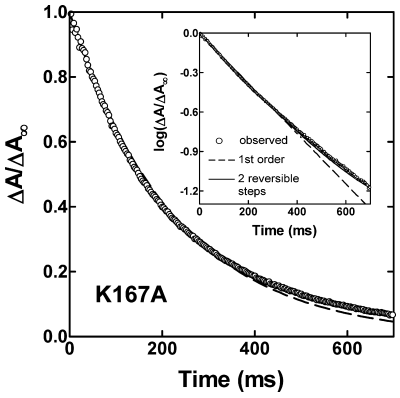

Figure 3. Anaerobic stopped-flow reduction of K167A by NADPH. After the rapid mixing, the reduction of the FMN cofactor (associated with decreases in A_{450}) of 10 μM K167A by 1 mM NADPH was followed over time (main figure). ΔA_∞ and ΔA are the actual A_{450} at time zero and any given time t, respectively, minus the final A_{450} upon completion of the reaction. A replot of $\log(\Delta A/\Delta A_\infty)$ versus time is shown in the inset. The observed data (○) were fitted for a first-order process (dashed line) and for a process consisting of two consecutive reversible steps (solid line) as shown in the boxed portion of Scheme 1.

ΔA_∞) (where ΔA_∞ and ΔA are the actual A_{450} at time zero and any given time t, respectively, minus the final A_{450} upon completion of the reaction) versus time is shown in the inset. The observed data can be fitted (the solid line in Figure 3 inset) according to two consecutive reversible reaction steps as shown in the boxed portion of Scheme 1, with k_1 at 8 mM^{-1} s^{-1} and k_2, k_3, and k_4 at values of 20, 31, and 0.3 s^{-1}, respectively. Correspondingly, the K_d (= k_2/k_1) for NADPH binding to the oxidized K167A enzyme was calculated to be 2.5 mM. A large portion of the initial time course followed a pseudo-first-order decay (dashed lines in Figure 3 main figure and inset), with the tail portion showing a slight deviation due to the inclusion of the k_4 step. However, the k_4 was 2 orders of magnitude slower than k_3. For an approximation, the much slower k_4 can be excluded from the boxed portion of Scheme 1, allowing the k_{obs} for the initial linear portion of the $\log(\Delta A/\Delta A_\infty)$ versus time plot to follow the relationship

$$\frac{1}{k_{obs}} = \frac{1}{k_3} + \frac{K_d}{k_3}\frac{1}{[NADPH]} \quad (3)$$

The experiment as shown in Figure 3 was repeated several times with the initial concentration of NADPH each time set at a different level (all being much higher than the total concentration of K167A), and the k_{obs} values of the initial pseudo-first-order phase are shown as a function of NADPH concentration (Figure 4, main figure). The double-reciprocal plot of k_{obs} versus initial NADPH concentration showed a linear line (Figure 4, inset), in consistency with eq 3. Accordingly, K_d and k_3 were determined to be 3.9 mM and 25 s^{-1}, respectively. These values were similar to the 2.5 mM and 31 s^{-1} for K_d and k_3, respectively, determined from the two-reversible-step fit of a single time course mentioned earlier for Figure 3 inset.

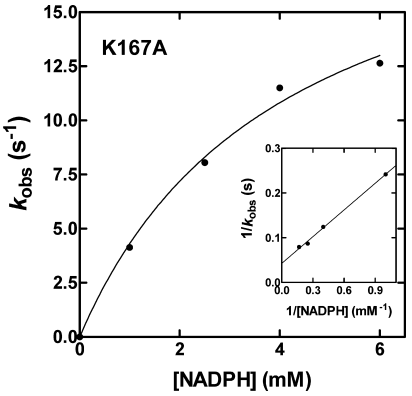

Figure 4. Dependence of the rate constant of K167A FMN cofactor reduction on NADPH concentration. The apparent first-order rate constant (k_{obs}) of the reduction of the FMN cofactor of 10 μM K167A by 1 mM NADPH was determined from the initial linear portion of the plot of $\log(\Delta A/\Delta A_\infty)$ versus time as shown in Figure 3 inset. The same experiment was repeated for three other NADPH concentrations. Values of k_{obs} so obtained are shown as a function of NADPH concentration (main figure) and as a double reciprocal plot (inset).

The same stopped-flow anaerobic experiments of the reduction of reductase-bound FMN by several levels of NADPH were also carried out using R15A. Similarly, values of k_{obs} for the initial linear portions of the $\log(\Delta A/\Delta A_\infty)$ versus time plots are shown as a function of NADPH concentration (Figure 5, main figure). Again, the double reciprocal plot of k_{obs} versus NADPH concentration followed a linear relationship (Figure 5, inset), allowing the determination of K_d and k_{cat} as 1.1 mM and 20 s^{-1}, respectively.

Scheme 1

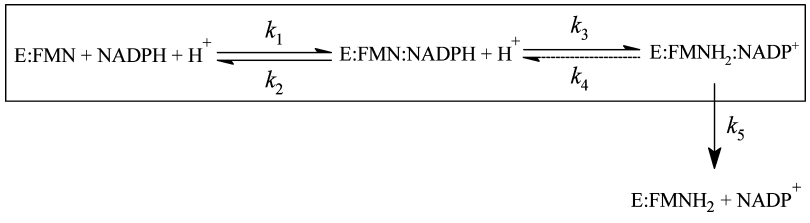

dx.doi.org/10.1021/bi3002314 | Biochemistry 2012, 51, 4880−4887

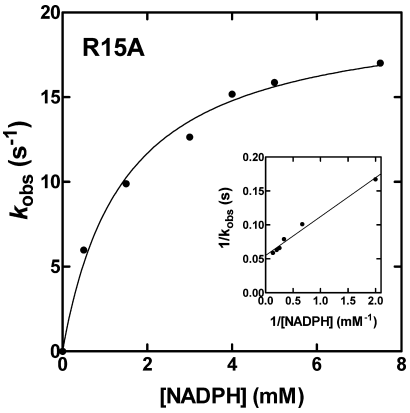

Figure 5. Dependence of the rate constant of R15A FMN cofactor reduction on NADPH concentration. The apparent first-order rate constants (k_{obs}) of the reduction of the FMN cofactor of 10 μM R15A FMN by 6 levels of NADPH were determined the same way as that described for Figures 3 and 4. Values of k_{obs} so obtained are shown as a function of NADPH concentration (main figure) and as a double reciprocal plot (inset).

Dependence of FRT and K167A Activities on NADH. It is known that the WT FRP has a low but measurable activity using NADH as a substrate.[21] We measured the dependence of K167A activity on NADH concentration (Figure 6, ●) and

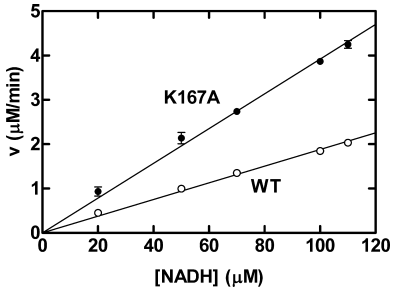

Figure 6. Dependence of reductase activity on NADH concentration. The steady-state initial velocities of 0.1 μM of WT FRP (○) and K167A (●) were determined at 50 μM FMN and various levels of NADH as indicated.

compared with that for the WT FRP (Figure 6, ○). From the slopes of the plots, k_{cat}/K_m of WT FRP and K167A were determined to be respectively 3.0×10^{-3} and 6.5×10^{-3} μM^{-1} s^{-1}.

DISCUSSION

The five residues initially targeted for investigation of their possible roles in NADPH binding and/or utilization by FRP were each mutated to an alanine, and the corresponding FRP variants were first characterized by steady-state initial velocity kinetic analyses (Table 2). In comparison with the wild-type FRP, R225A showed very little changes in $K_{m,NADPH}$ and k_{cat}. Less than 5-fold increases in $K_{m,NADPH}$ or decreases in k_{cat} were found for R133A and N134A. In contrast, values of the $K_{m,NADPH}$ for K167A and R15A were apparently increased markedly to the extents to show a nearly linear dependence of their initial velocity on NADPH concentration up to 100 and 50 μM tested for K167A and R15A, respectively (Figure 2). Results available to this point strongly support an important role in NADPH binding by K167 and R15. Values of the $k_{cat}/K_{m,NADPH}$ for K167A and R15A were also determinable to be 0.025 and 0.012 μM^{-1} s^{-1}, respectively, from results shown in Figure 2. Both are greatly reduced from the 2.7 μM^{-1} s^{-1} of the wild-type FRP. However, individual values of $K_{m,NADPH}$ and k_{cat} could not be determined for these two FRP variants from the steady-state NADPH titration experiments. Therefore, these two FRP variants were subjected to additional kinetic analyses.

NADPD in addition to NADPH was used for steady-state initial velocity measurements for K167A, R15A, and the native FRP. Again, due to a nearly linear dependence of initial velocities on NADPD concentrations, values of $k_{cat}/K_{m,NADPD}$ could be determined but not for individual values of k_{cat} and $K_{m,NADPD}$ for K167A or R15A (Figure 2). Accordingly, steady-state deuterium isotope effects $^{D}(V/K)$ of 6.3 ± 1.6 and 7.4 ± 0.3 were found for K167A and R15A, respectively, in comparison with 1.0 ± 0.2 for the native FRP. These results were further analyzed according to the full Scheme 1 (including all the steps k_1 through k_5), in which k_3 and k_4 are deuterium isotope-sensitive steps. Also the following relationships exist:

$$^{D}(V/K) = \frac{^{D}k_3 + \frac{k_{3H}}{k_2} + \frac{k_{4H}}{k_5}{}^{D}K_{eq}}{1 + \frac{k_{3H}}{k_2} + \frac{k_{4H}}{k_5}} \quad (4)$$

$$^{D}K_{eq} = \frac{k_{3H}/k_{3D}}{k_{4H}/k_{4D}} = \frac{^{D}k_3}{^{D}k_4} \quad (5)$$

where $^{D}k_3 = k_{3H}/k_{3D}$ and $^{D}k_4 = k_{4H}/k_{4D}$. If the isotope-sensitive step is reversible, then the $^{D}K_{eq}$ equilibrium isotope effect is usually equal to 1, and $^{D}k_3$ could be as high as 7 when k_3 is the sole rate-limiting step in the forward reaction. According to eq 4, $^{D}(V/K)$ can be minimized to near unity when $k_{3H} \gg k_2$ and $k_{4H} \gg k_5$ but is increased to near the value of $^{D}k_3$ if $k_{3H} \ll k_2$ and $k_{4H} \ll k_5$. The former was observed with the wild-type enzyme whereas the latter was found for R15A and K167A. Therefore, the mutation of each of R15 and K167 to an alanine resulted in marked increases in the dissociation rate constants for NADPH (i.e., k_2) and $NADP^+$ (i.e., k_5) in relation to k_3 and k_4, respectively. The finding that $^{D}(V/K)$ was near 7 for K167A and R15A also indicates that k_2 and k_5 were much faster than k_3, making k_3 the sole rate-limiting step for these two FRP variants. All these findings are consistent with and further support the earlier conclusion that K167 and R15 were important for the binding of the pyridine nucleotide.

NADPH binding by K167A and R15A and the rates of their FMN cofactor reduction by NADPH were examined by anaerobic stopped-flow studies. As shown in Figure 3 and inset, the observed ΔA time course (shown as $\Delta A/\Delta A_\infty$) for K167A deviated slightly from the theoretical first-order kinetics. The same general pattern was observed for K167A and R15A at several NADPH concentrations tested. Three possibilities were considered. First, assuming that K167A and R15A are similar to WT FRP in having a K_d of 0.2 μM for the FMN cofactor binding,[16] the 10 μM reductase samples after mixing in the anaerobic stopped-flow experiments should contained about 12% free FMN. But, the analysis of the observed reduction of FMN was based on ΔA_{450} instead of absolute A_{450}. Since the enzymatic reduction of the bound FMN was much faster than the nonenzymatic reduction of free FMN by NADPH, the absorption at 450 nm due to free FMN should essentially be constant during the time period of data collection. Hence, the observed $\Delta A/\Delta A_\infty$ time course should reflect the true kinetics of the enzymatic reaction. The slight deviation from first-order

dx.doi.org/10.1021/bi3002314 | Biochemistry 2012, 51, 4880−4887

kinetics in the $\Delta A/\Delta A_\infty$ time course was unlikely caused by a low level of free FMN. Second, WT FRP also undergoes a monomer−dimer equilibrium with a K_d of 1.8 μM.[16] Our previous *in silico* mutations and energetic analyses led us to identify a number of residues that could be important in the dimer formation of FRP.[22] K167 and R15 are not among them. Hence, their mutations to alanine were unlikely to change the monomer−dimer equilibrium in any significant way. Assuming the same K_d of 1.8 μM in dimerization for K167A and R15A, the monomeric reductase should be at 2.6 μM at a total concentration of 10 μM for the reductase as that used in the stopped-flow experiments. The deviation of the observed ($\Delta A/\Delta A_\infty$) time course from first-order decay could be a consequence of the nonidentical rates of FMN cofactor reduction by the monomeric and the dimeric enzymes. We cannot eliminate this possibility. But, FRP samples with 20−30% monomer contents did not show any multiphasic behaviors in our previous equilibrium titration experiments.[24] Third, we have previously shown that the conversions between E:FMN:NADPH and E:FMNH$_2$:NADP$^+$ complexes (in which E is the apoenzyme and FMN is the bound flavin cofactor) are reversible.[24] When the step associated with k_4 is included in the boxed portion of Scheme 1, the theoretical time course of ($\Delta A/\Delta A_\infty$) is no longer a simple first-order process. In fact, the observed time course as shown in Figure 3 can be satisfactorily fitted by a two-step reversible reaction (Figure 3 inset). We consider this third possibility the most likely cause for the slight deviations from first-order kinetics for K167A and R15A in the anaerobic reduction of the bound FMN cofactor. The 0.3 s^{-1} k_4 revealed by fitting the data in Figure 3 to a two-step reversible reaction scheme was 2 orders of magnitude slower than the 31 s^{-1} k_3. For an approximation, when the much slower k_4 is excluded from consideration, k_{obs} values can be obtained from the initial linear portions of the log($\Delta A/\Delta A_\infty$) versus time plots of the data from stopped-flow anaerobic reduction experiments for K167A and R15A such as that shown in Figure 3 inset. Moreover, the double-reciprocal plots of k_{obs} versus NADPH concentration should be linear according to eq 3. Indeed, linear plots were obtained as shown in the insets of Figures 4 and 5, allowing the determination of K_d and k_3 as respectively 3.9 mM and 25 s^{-1} for K167A and 1.1 mM and 20 s^{-1} for R15A. The values of K_d and k_3 determined in such a way for K167A were quite similar to 2.5 mM and 31 s^{-1}, respectively, determined from the two-reversible-step fit of a single time course shown in Figure 3 inset.

The values of k_3 for K167A and R15A were quite similar to the k_{cat} of WT FRP at 24 s^{-1} (Table 2), establishing that neither K167 nor the R15 was important to the hydride transfer from NADPH to the FMN cofactor or the subsequent reduction of the flavin substrate by the reduced FMN cofactor. On the other hand, the values of K_d for NADPH binding by K167A and R15A were 4 orders of magnitude higher than that for the WT FRP at 0.4 μM.[24] The hugely increased K_d values for K167A and R15A clearly showed that both K167 and R15 residues were critical to the binding of the pyridine nucleotide substrate by the reductase. These findings also indicate that the markedly reduced $k_{cat}/K_{m,NADPH}$ values for K167A and R15A as shown in Table 2 were primarily due to the increased $K_{m,NADPH}$ rather than reduced k_{cat}.

FRP has a low but measurable activity with NADH.[21] While K167A showed markedly reduced binding affinity of NADPH and the $k_{cat}/K_{m,NADPH}$ value, the K167 to alanine mutation resulted in even a slight higher value of $k_{cat}/K_{m,NADH}$ than that of WT FRP (Figure 6). Such a finding further indicated that the K167 residue was important in a specific interaction with NADPH.

Results from the present investigations strongly support the hypothesis that both K167 and R15 play essential roles in NADPH binding to FRP. We speculate that an electrostatic interaction may exist between a negatively charged site in NADPH and the positively charged side chains of K167 and R15. Such a notion is consistent with the finding that mutations of K167 or R15 greatly reduced the NADPH binding affinity but did not affect the hydride transfers. Our findings also suggest that these two residues in other homologous proteins, such as in NfsA and SNrA, may have similar functional roles.

AUTHOR INFORMATION

Corresponding Author

*E-mail dtu@uh.edu; Ph (713) 743-8359.

Funding

Funding is made possible by an endowment of the John and Rebecca Moores Professorship and by the National Science Council, Taiwan, ROC.

Notes

The authors declare no competing financial interest.

ACKNOWLEDGMENTS

S.C.T. is grateful to an endowment of the John and Rebecca Moores Professorship and the funding from National Science Council, Taiwan, ROC.

ABBREVIATIONS

FRP, NADPH−flavin oxidoreductase; DTT, dithiothreitol; NADPD, (4R)-[4-^{2}H]-NADPH.

REFERENCES

(1) Hallé, F., and Meyer, J.-M. (1992) Iron release from ferrisiderophores. A multi-step mechanism involving a NADH/FMN oxidoreductase and a chemical reduction by FMNH$_2$. *Eur. J. Biochem. 209*, 621−627.

(2) Fontecave, M., Eliasson, R., and Reichard, P. (1987) NAD(P)-H:flavin oxidoreductase of *Escherichia coli*. A ferric iron reductase participating in the generation of the free radical of ribonucleotide reductase. *J. Biol. Chem. 262*, 12325−12331.

(3) Quandt, K. S., Xu, F., Chen, P., and Hultquist, D. E. (1991) Evidence that the protein components of bovine erythrocyte green heme binding protein and flavin reductase are identical. *Biochem. Biophys. Res. Commun. 178*, 315−321.

(4) Gaudu, P., Touati, D., Nivière, V., and Fontecave, M. (1994) The NAD(P)H:flavin oxidoreductase from *Escherichia coli* as a source of superoxide radicals. *J. Biol. Chem. 269*, 8182−8188.

(5) Tu, S.-C. (2001) Reduced flavin: donor and acceptor enzymes and mechanisms of channeling. *Antioxid. Redox Signaling 3*, 881−897.

(6) Tu, S. C. (2008) Activity coupling and complex formation between bacterial luciferase and flavin reductases. *Photochem. Photobiol. Sci. 7*, 183−188.

(7) Gerlo, E., and Charlier, J. (1975) Identification of NADH-specific and NADPH-specific FMN reductases in *Beneckea harveyi*. *Eur. J. Biochem. 57*, 461−467.

(8) Jablonski, E., and DeLuca, M. (1977) Purification and properties of the NADH and NADPH specific FMN oxidoreductases from *Beneckea harveyi*. *Biochemistry 16*, 2932−2936.

(9) Michaliszyn, G. A., Wing, S. S., and Meighen, E. A. (1977) Purification and properties of a NAD(P)H:flavin oxidoreductase from the luminous bacterium *Beneckea harveyi*. *J. Biol. Chem. 252*, 7495−7499.

(10) Watanabe, H., and Hastings, J. W. (1982) Specificities and properties of three reduced pyridine nucleotide-flavin mononucleotide reductases coupling to bacterial luciferase. *Mol. Cell. Biochem. 44*, 181–187.
(11) Jeffers, C. E., and Tu, S.-C. (2001) Differential transfers of reduced flavin cofactor and product by bacterial flavin reductase to luciferase. *Biochemistry 40*, 1749–1754.
(12) Lei, B., and Tu, S.-C. (1998) Mechanism of reduced flavin transfer from *Vibrio harveyi* NADPH-FMN oxidoreductase to luciferase. *Biochemistry 37*, 14623–14629.
(13) Jeffers, C. E., Nichols, J. C., and Tu, S.-C. (2003) Complex formation between *Vibrio harveyi* luciferase and monomeric NADPH:FMN oxidoreductase. *Biochemistry 42*, 529–534.
(14) Low, J. C., and Tu, S.-C. (2003) Energy transfer evidence for in vitro and in vivo complexes of *Vibrio harveyi* flavin reductase P and luciferase. *Photochem. Photobiol. 77*, 446–452.
(15) Lei, B., Liu, M., Huang, S., and Tu, S.-C. (1994) *Vibrio harveyi* NADPH-flavin oxidoreductase: cloning, sequencing and overexpression of the gene and purification and characterization of the cloned enzyme. *J. Bacteriol. 176*, 3552–3558.
(16) Liu, M., Lei, B., Ding, Q., Lee, J. C., and Tu, S.-C. (1997) *Vibrio harveyi* NADPH:FMN oxidoreductase: preparation and characterization of the apoenzyme and monomer-dimer equilibrium. *Arch. Biochem. Biophys. 337*, 89–95.
(17) Tanner, J. J., Lei, B., Tu, S.-C., and Krause, K. L. (1996) Flavin reductase P: structure of a dimeric enzyme that reduces flavin. *Biochemistry 35*, 13531–13539.
(18) Kobori, T., Sasaki, H., Lee, W. C., Zenno, S., Saigo, K., Murphy, M. E. P., and Tanokura, M. (2001) Structure and site-directed mutagenesis of a flavoprotein from *Escherichia coli* that reduces nitrocompounds. *J. Biol. Chem. 276*, 2816–2823.
(19) Nokhbeh, M. R., Boroumandi, S., Pokorny, N., Koziarz, P., Paterson, E. S., and Lambert, I. B. (2002) Identification and characterization of SnrA, an inducible oxygen-insensitive nitroreductase in *Salmonella enterica* serovar Typhimurium TA1535. *Mutat. Res., Fundam. Mol. Mech. Mutagen. 508*, 59–70.
(20) Zenno, S., Kobori, T., Tanokura, M., and Saigo, K. (1998) Purification and characterization of NfrA1, a *Bacillus subtilis* nitro/flavin reductase capable of interacting with the bacterial luciferase. *Biosci. Biotechnol. Biochem. 62*, 1978–1987.
(21) Wang, H., Lei, B., and Tu, S.-C. (2000) *Vibrio harveyi* NADPH-FMN oxidoreductase Arg203 as a critical residue for NADPH recognition and binding. *Biochemistry 39*, 7813–7819.
(22) Jawanda, N., Ebalunode, J., Gribenko, A., Briggs, J., Lee, J. C., and Tu, S.-C. (2008) A single-residue mutation destabilizes *Vibrio harveyi* flavin reductase FRP dimer. *Arch. Biochem. Biophys. 472*, 51–57.
(23) Sem, D. S., and Kasper, C. B. (1992) Geometric relationship between the nicotinamide and isoalloxazine rings in NADPH-cytochrome P-450 oxidoreductase: implications for the classification of evolutionarily and functionally related flavoproteins. *Biochemistry 31*, 3391–3398.
(24) Lei, B., Wang, H., Yu, Y., and Tu, S.-C. (2005) Redox potential and equilibria in the reductive half-reaction of *Vibrio harveyi* NADPH-FMN oxidoreductase. *Biochemistry 44*, 261–267.
(25) Zenno, S., Koike, H., Kumar, A., Jayaraman, R., Tanokura, M., and Saigo, K. (1996) Biochemical characterization of NfsA, the *Escherichia coli* major nitroreductase exhibiting a high amino acid sequence homology to Frp, a *Vibrio harveyi* flavin oxidoreductase. *J. Bacteriol. 178*, 4508–4514.